Fibulin-4 conducts proper elastogenesis via interaction with cross-linking enzyme lysyl oxidase

Masahito Horiguchi[a], Tadashi Inoue[b,c], Tetsuya Ohbayashi[d], Maretoshi Hirai[e], Kazuo Noda[c,f], Lihua Y. Marmorstein[g], Daisuke Yabe[h], Kyoko Takagi[c,i], Tomoya O. Akama[c], Toru Kita[a,j], Takeshi Kimura[a], and Tomoyuki Nakamura[c,1]

Departments of [a]Cardiovascular Medicine and [f]Plastic and Reconstructive Surgery, Graduate School of Medicine, Kyoto University, Kyoto, 606-8507, Japan; Departments of [b]Skin Regenerative Medicine and [c]Pharmacology, Kansai Medical University, Moriguchi, Osaka, 570-8506, Japan; [d]Division of Laboratory Animal Science, Research Center for Bioscience and Technology, Tottori University, Yonago, Tottori, 683-8503, Japan; [e]Skaggs School of Pharmacy and Pharmaceutical Sciences, University of California, San Diego, La Jolla, CA 92093; [g]Departments of Ophthalmology and Vision Science, and Physiology, University of Arizona, Tucson, AZ 85711; [h]Department of Diabetes and Clinical Nutrition, Kansai Electric Power Hospital, Osaka, 553-0003, Japan; [i]Rohto Pharmaceutical Company Limited, Kyoto, 619-0216, Japan; and [j]Kobe City Medical Center General Hospital, Kobe, Hyogo, 650-0046, Japan

Edited by Yoshito Kaziro, Kyoto University, Kyoto, Japan, and approved September 18, 2009 (received for review July 22, 2009)

Great arteries, as well as lungs and skin, contain elastic fibers as important components to maintain their physiological functions. Although recent studies have revealed that a glycoprotein fibulin-4 (FBLN4) is indispensable for the assembly of mature elastic fibers, it remains to be elucidated how FBLN4 takes part in elastogenesis. Here, we report a dose-dependent requirement for FBLN4 in the development of the elastic fibers in arteries, and a specific role of FBLN4 in recruiting the elastin-cross-linking enzyme, lysyl oxidase (LOX). Reduced expression of *Fbln4*, which was achieved with a smooth muscle-specific Cre-mediated gene deletion, caused arterial stiffness. Electron-microscopic examination revealed disorganized thick elastic laminae with aberrant deposition of elastin. Aneurysmal dilation of the ascending aorta was found when the *Fbln4* expression level was reduced to an even lower level, whereas systemic *Fbln4* null mice died perinatally from rupture of the diaphragm. We also found a specific interaction between FBLN4 and the propeptide of LOX, which efficiently promotes assembly of LOX onto tropoelastin. These data suggest a mechanism of elastogenesis, in which a sufficient amount of FBLN4 is essential for tethering LOX to tropoelastin to facilitate cross-linking.

development | elastin | extracellular matrix

Elasticity is an important characteristic for many vital organs such as the great arteries, lungs, and skin (1). To maintain their physiological function, these organs need to undergo repeated cycles of extension and contraction. However, aging leads to loss of elasticity in these organs, resulting in loose skin and pathological conditions such as aortic aneurysm, arteriosclerosis, and lung emphysema (2, 3). Elasticity is provided by the abundant elastic fibers contained in these tissues. The major components of elastic fibers are polymerized elastin and microfibrils (1). Microfibrils are thin filaments 10–15 nm in diameter, mainly composed of fibrillin-1 and fibrillin-2 (4, 5). These filaments serve as a scaffold to assemble tropoelastin, i.e., elastin monomer (6). Tropoelastin is a 60- to 70-kDa secreted protein and contains lysine-rich sequences (7). In normal elastogenesis, it is proposed that tropoelastin monomers form small aggregates by self-assembly, a process called coacervation, and these aggregates are then transported onto microfibrils followed by cross-linking of lysine residues, catalyzed by lysyl oxidase (LOX), to form mature elastic fibers (8).

Several other proteins, such as microfibril associated glycoproteins (MAGPs) (9, 10), elastin microfibril interface located proteins (EMILINs) (11, 12), fibronectin (13, 14), and latent TGF-β binding proteins (LTBPs) (15, 16), also contribute to elastogenesis. Fibulins (FBLNs) are proteins recently reported to have important roles in elastogenesis. So far, the FBLN family consists of seven members, which share tandem arrays of calcium-binding (cb)EGF-like domains and a conserved carboxy-terminal domain (17, 18). Among these members, FBLN3, 4, and 5 are 50- to 60-kDa secreted proteins that share particularly high homology to each other (19). Recent studies using genetically engineered mice revealed that FBLN3, 4, and 5 are indispensable for normal elastogenesis. FBLN3 was identified as a protein overexpressed in fibroblasts derived from a patient with Werner syndrome (20). Mutations in the human *FBLN3* gene are associated with the eye diseases Doyne honeycomb retinal dystrophy and Malattia Leventinese (21). *Fbln3*-deficient mice show defective elastogenesis mainly in connective tissue fascia, leading to inguinal hernias and protrusion of xiphoid process without obvious manifestation in the vascular system (22). Developmental arteries and neural crest EGF-like protein (DANCE, also called FBLN5) is another member of the FBLN family, abundantly present in developing arteries (19, 23). *Dance*-deficient mice show stiff and tortuous aortae, emphysematous lungs, and loose skin, indicating that DANCE has an essential role in elastogenesis (24, 25). Our previous studies revealed that recombinant DANCE protein promotes elastic fiber assembly in serum-free cell culture by recruiting tropoelastin to microfibrils (26). Mutations in the *DANCE* gene have been implicated in human diseases, i.e., age-related macular degeneration and cutis laxa syndrome (27–29). FBLN4 was cloned as a new matrix protein from a melanoma cDNA library (30). Recently, *Fbln4*-deficient mice were described (31). These mice have tortuous aortae and emphysematous lungs, with severe disruption in elastic tissues. Although FBLN4 is suggested to be involved in some pathological conditions such as cutis laxa, aneurysm, and osteoarthritis (32, 33), the role of FBLN4 in postnatal development has not been fully elucidated, because *Fbln4* null mutations are perinatally lethal. The mechanism by which FBLN4 contributes to elastogenesis is not known, although elastin cross-links are largely lost in *Fbln4*-deficient mice (31).

LOXs are copper-requiring amine oxidases that catalyze cross-linking of elastin molecules. They are composed of five members: LOX and LOX-like 1–4 (LOXL1–4) (34), among which LOX and LOXL1 are most similar and comprise a subfamily. They are secreted as inactive proenzymes, 50-kDa proLOX and 60-kDa proLOXL1, respectively, containing a glycosylated N-terminal propeptide domain followed by the catalytic domain. The propeptides of the proenzymes are eventually cleaved by proteases, such as bone morphogenic protein (BMP)1 and tolloid-like (TLL)1 (35, 36), producing mature 32-kDa LOX or 31-kDa LOXL1. The propeptides of LOX and LOXL1 are reported to be required for targeting mature enzymes on elastic fibers (37), but the precise

Author contributions: M. Horiguchi, T.O., M. Hirai, T. Kita, T. Kimura, and T.N. designed research; M. Horiguchi, T.I., T.O., M. Hirai, K.N., and K.T. performed research; L.Y.M. and D.Y. contributed new reagents/analytic tools; M. Horiguchi, T.I., T.O., M. Hirai, K.N., and T.N. analyzed data; and M. Horiguchi, T.O.A., and T.N. wrote the paper.

The authors declare no conflict of interest.

This article is a PNAS Direct Submission.

[1]To whom correspondence should be addressed. E-mail: nakamtom@takii.kmu.ac.jp.

This article contains supporting information online at www.pnas.org/cgi/content/full/0908268106/DCSupplemental.

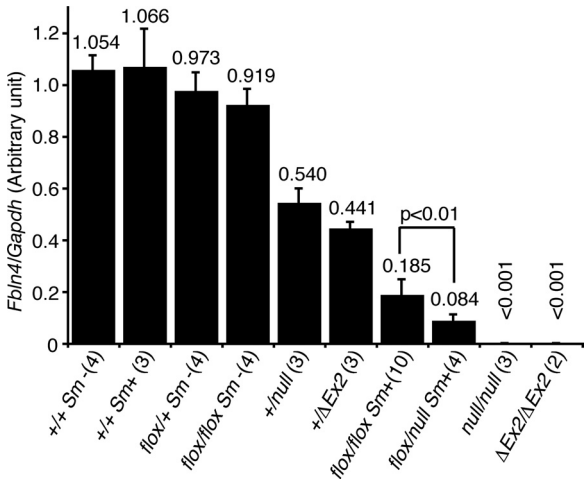

Fig. 1. Quantitative PCR of neonatal aortae. Total RNA of mouse neonatal aortae was extracted and reverse transcribed to cDNA, followed by quantitative PCR. Relative expression level of *Fbln4* in a wild-type mouse was defined as 1.0. Numbers of studied mice are indicated in parentheses. The expression of *Fbln4* was suppressed effectively in $Fbln4^{flox/null}$ *Sm*+ and $Fbln4^{flox/flox}$ *Sm*+ mice, with reduced expression levels of 8.4 and 18.5%, respectively.

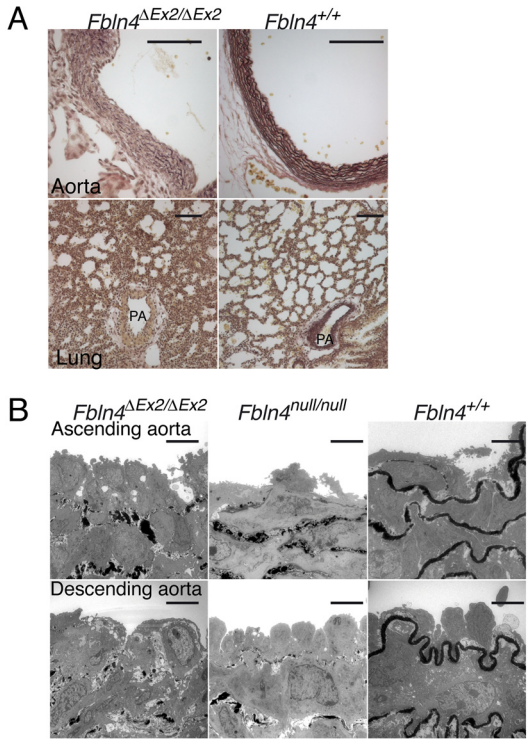

Fig. 2. Systemic deletion of *Fbln4* exon 2 leads to complete disruption of elastic tissues. (*A*) EVG staining of neonatal aorta shows defective development of elastic lamina (*Upper*), and that of lung shows defective distal airways (*Lower*) of $Fbln4^{\Delta Ex2/\Delta Ex2}$ neonate. A small branch of the pulmonary artery (PA) was also affected. (Scale bar, 100 μm.) (*B*) TEM of neonatal arteries. $Fbln4^{\Delta Ex2/\Delta Ex2}$ neonates show severely disrupted elastic laminae, similar to those of previously reported $Fbln4^{null/null}$ mice. (Scale bar, 5 μm.)

mechanism has not been elucidated. *Lox*-deficient mice have large defects in their diaphragms, have markedly tortuous aortae with severely disrupted elastic laminae, and die perinatally (38, 39).

To elucidate the precise role of FBLN4 in the development of elastic fibers in arteries, we generated mice harboring floxed *Fbln4* alleles and crossed them with *Sm22-Cre* mice that express Cre recombinase in smooth muscle cells. The aortae of $Fbln4^{flox/flox}$ *Sm*+ mice are stiff, and the elastic laminae are disorganized with aberrant deposition of elastin. Severe aneurysmal dilatation of the ascending aortae was found in $Fbln4^{flox/null}$ *Sm*+ mice, showing a dose-dependent requirement for FBLN4 in aorta development. We also report a specific interaction between FBLN4 and the propeptide of LOX, which facilitates assembly of LOX on tropoelastin. These results imply that FBLN4 acts as an indispensible adaptor between proLOX and elastin to facilitate proper maturation of elastic fibers.

Results

Generation of *Fbln4* Conditional Knockout Mice. *Fbln4* conditional knockout mice were generated as described in *Methods* and in Fig. S1*A*. The Cre-loxP-mediated recombination generated the "Δ*Ex2*" allele, causing a frameshift and producing a stop codon in exon 3, resulting in a short peptide of 15-aa length after cleavage of the signal peptide (Fig. S1*B*). Successfully targeted ES cells and F1 mice were identified by Southern blotting (Fig. S1 *C* and *D*, respectively). Primer sequences used to amplify the probe are shown in Table S1. The *Fbln4* allele of knockout mice previously reported (31) will be designated hereafter as the "*null*" allele for clarity.

To confirm that Δ*Ex2* allele cannot produce functional FBLN4 protein, we monitored *Fbln4* mRNA and FBLN4 protein levels in $Fbln4^{\Delta Ex2/\Delta Ex2}$ mice. The expression of *Fbln4* mRNA and FBLN4 protein were abolished in $Fbln4^{\Delta Ex2/\Delta Ex2}$ mice (Fig. 1; Fig. S2*A*). These mice died just after birth with severe diaphragmatic hernias (Fig. S3 *A* and *B*) and tortuous aortae (Fig. S3*C*). Elastica van Gieson (EVG) staining showed complete disarrangement of aortic elastic laminae and impaired development of distal airways (Fig. 2*A*). Transmission electron microscopy (TEM) showed that elastogenesis was abolished in the entire aorta in $Fbln4^{\Delta Ex2/\Delta Ex2}$ mice, a phenotype identical to that of $Fbln4^{null/null}$ mice (Fig. 2*B*). These results indicate that deletion of exon 2 of *Fbln4* extinguishes the expression of functional protein.

To investigate the tissue-specific role of FBLN4 in arteries, smooth muscle-specific conditional knockout mice were generated by crossing $Fbln4^{flox/+}$ mice with mice expressing Cre recombinase under control of the *Smooth Muscle Protein 22α* (*Sm22α*, also known as *Tagln*) gene promoter (40). The expression of *Sm22α* is detected in the dorsal aorta as early as in 9.5 days postcoitus (dpc) (41). Examination at 14.5 dpc of indicator mice crossed with *Sm22α-Cre* mice confirmed that the Cre recombinase is expressed in the entire layer of the developing aorta (Fig. S2*B*). Western blotting of $Fbln4^{flox/flox}$ *Sm*+ embryos at 16.5 dpc showed that the expression of FBLN4 protein was largely abolished in the aorta or umbilicus, whereas its expression level was comparable with wild type in the lung, skin, skeletal muscle, and kidney (Fig. S2*C*). To minimize the effect of the residual FBLN4, we also generated compound heterozygous mutant mice with a $Fbln4^{flox/null}$ *Sm*+ genotype. Quantitative PCR analysis showed that the expression of *Fbln4* mRNA in neonatal aortae of $Fbln4^{flox/null}$ *Sm*+ or $Fbln4^{flox/flox}$ *Sm*+ mice was significantly decreased to 8.4 ± 2.7% or 18.5 ± 6.3% of that of wild-type mice, respectively (Fig. 1). These results indicate that Cre recombinase expressed under *Sm22α* promoter successfully disrupted the *Fbln4* gene in developing arteries.

Dose-Dependent Requirement for FBLN4 in the Development of Aortic Elastic Laminae After Birth. Phenotypes of $Fbln4^{flox/null}$ *Sm*+ and $Fbln4^{flox/flox}$ *Sm*+ mice were examined by comparing them with $Fbln4^{flox/flox}$ *Sm*− or $Fbln4^{+/+}$ *Sm*+ mice. All of these mice grew normally, were fertile, and their survival was comparable up to 1 year.

Aortography revealed severe ascending aortic aneurysms in $Fbln4^{flox/null}$ *Sm*+ mice accompanied by aortic valve insufficiency, whereas the aortic arches of $Fbln4^{flox/flox}$ *Sm*+ mice were only slightly elongated (Fig. 3*A*). Macroscopic examination of $Fbln4^{flox/null}$ *Sm*+ mice confirmed severe dilatation of the as-

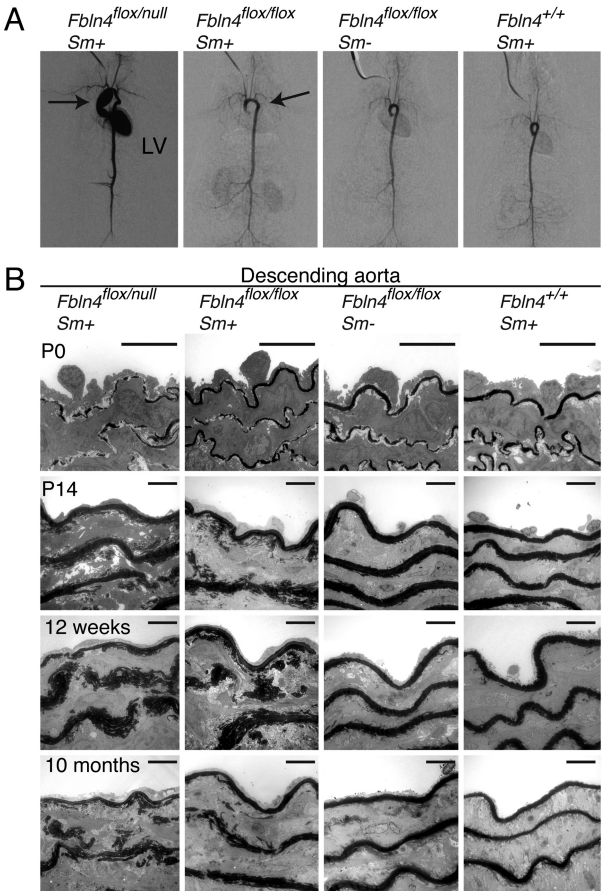

Fig. 3. Disrupted elastogenesis in the aortae of *Fbln4*$^{flox/null}$ and *Fbln4*$^{flox/flox}$ mice. (*A*) Aortography of 1-year-old mice. *Fbln4*$^{flox/null}$ *Sm+* mice showed markedly enlarged ascending aortae and tortuous descending aortae. Left ventricle (LV) was stained, which may be due to aortic valve insufficiency. *Fbln4*$^{flox/flox}$ *Sm+* mice showed elongated aortic arch. (*B*) TEM of aortae at P0, P14, 12 weeks, and 10 months. Elastic laminae of *Fbln4*$^{flox/null}$ *Sm+* mice were already affected at P0, whereas those of *Fbln4*$^{flox/flox}$ *Sm+* mice were not. Abnormal disrupted elastic laminae were observed at P14 in *Fbln4*$^{flox/flox}$ *Sm+* mice. Note that elastic laminae are thicker and spongy in conditional knockout mice, and that there are aberrant deposits of elastin in the interlaminar spaces. (Scale bar, 10 μm.)

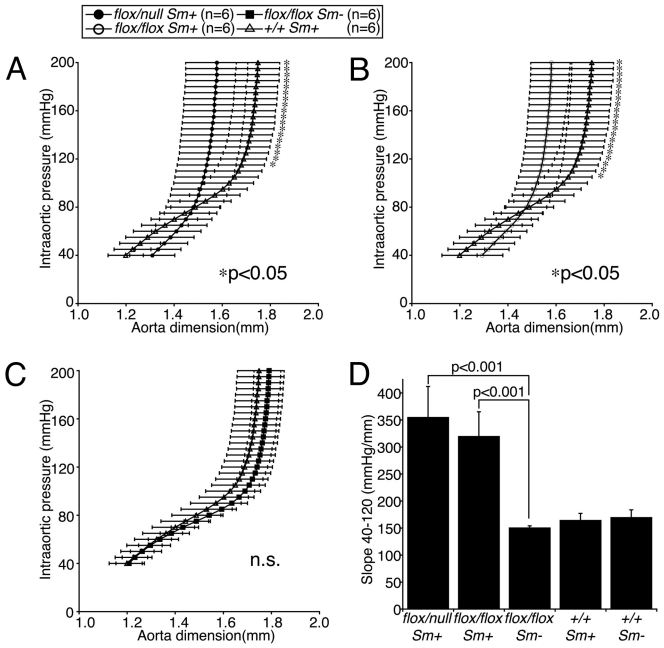

Fig. 4. Loss of elasticity in aortae of *Fbln4* conditional knockout mice. (*A–C*) Pressure-diameter relationships of *Fbln4* conditional knockout mice. Twelve-week-old mice were used for these analyses. (*D*) Slopes of pressure-diameter curves. Aortae of *Fbln4*$^{flox/null}$ *Sm+* and *Fbln4*$^{flox/flox}$ *Sm+* mice were significantly stiffer than those of *Fbln4*$^{flox/flox}$ *Sm−* mice or *Fbln4*$^{+/+}$ *Sm+* mice, whereas these two control mice showed no significant difference. Data are represented as means ± SD.

cending aorta, from the aortic root to just distal to the branching point of the brachiocephalic artery (Fig. S4 *A* and *B*). There was no aortic stenosis. Left ventricular hypertrophy was present in *Fbln4*$^{flox/null}$ *Sm+* mice, which may be due to aortic insufficiency, because regurgitation of the contrast media into the left ventricle was observed (Fig. S4*C*).

To investigate the development of elastic tissues in the aorta, specimens of descending aortae were examined with TEM at postnatal days (P)0, P14, 12 weeks, and 10 months (Fig. 3*B*). The aortic laminae of *Fbln4*$^{flox/null}$ *Sm+* mice were already disrupted at P0, although continuous thin layers of elastic lamina were formed in *Fbln4*$^{flox/flox}$ *Sm+* mice and control mice. At P14, the elastic laminae of both *Fbln4*$^{flox/null}$ *Sm+* and *Fbln4*$^{flox/flox}$ *Sm+* mice were disrupted; they were fragmented and of spongy appearance, and clumps of elastin were not integrated into compact lamellar structure. Thereafter, the laminae failed to develop properly, resulting in markedly fragmented and spongy elastic laminae with some elastin clumps scattered in interlaminar spaces. These findings were also observed in the ascending aortae (Fig. S4*D*). The results from *Fbln4*$^{flox/flox}$ *Sm+* mice indicate that the residual (18.5%) expression of *Fbln4* in arteries is sufficient for embryonic development of elastic laminae, but is insufficient to support the development of elastic laminae after birth. The results from *Fbln4*$^{flox/null}$ *Sm+* mice indicate that less (8.4%) expression of *Fbln4* in the developing aorta not only falls short of organizing elastic laminae in embryogenesis, but also leads to ascending aortic aneurysm.

Impaired Elastic Properties of Aortae of Conditional Knockout Mice. To assess the elasticity of these aortae, pressure-diameter relationships were investigated with *ex vivo* experiments of 12-week-old mice. The acquired curves of both *Fbln4*$^{flox/null}$ *Sm+* and *Fbln4*$^{flox/flox}$ *Sm+* mice were much steeper than those of control mice, indicating that these aortae are significantly less distensible (Fig. 4 *A* and *B*). The curves for control mice did not differ significantly each other (Fig. 4*C*). In the range of physiological pressure, i.e., 40- to 120-mm Hg, the slopes of the pressure-diameter curves for *Fbln4*$^{flox/null}$ *Sm+* and *Fbln4*$^{flox/flox}$ *Sm+* mice were significantly larger than those of the control groups (Fig. 4*D*). These results indicate that disruption of *Fbln4* leads not only to morphologically, but also to physiologically impaired aortic elastic laminae, resulting in significantly stiff aortae.

FBLN4, but Not DANCE/FBLN5, Specifically Interacts with the Propeptide of LOX via Its Amino Terminus Domain. Because *Fbln4* null mouse tissues are reported to contain largely reduced amount of desmosine (31), we hypothesized that FBLN4 may act on the expression or function of LOX, a cross-linking enzyme of elastin. The expression level of neither *Lox* mRNA nor LOX protein was affected in *Fbln4* conditional knockout mice aortae (Fig. S5). Therefore, we investigated the interaction of FBLN4 and LOX by in vitro binding assays. Myc-tagged LOX proteins were incubated with FLAG-tagged FBLN4 or DANCE proteins. Each mixture was subjected to immunoprecipitation with anti-FLAG antibody, and then, Myc-tagged LOX associated with the FLAG-tagged proteins were detected by Western blotting. This examination revealed that FBLN4 interacts with LOX, whereas DANCE does not (Fig. 5*A*).

To identify the binding domain, FBLN4 protein was divided into

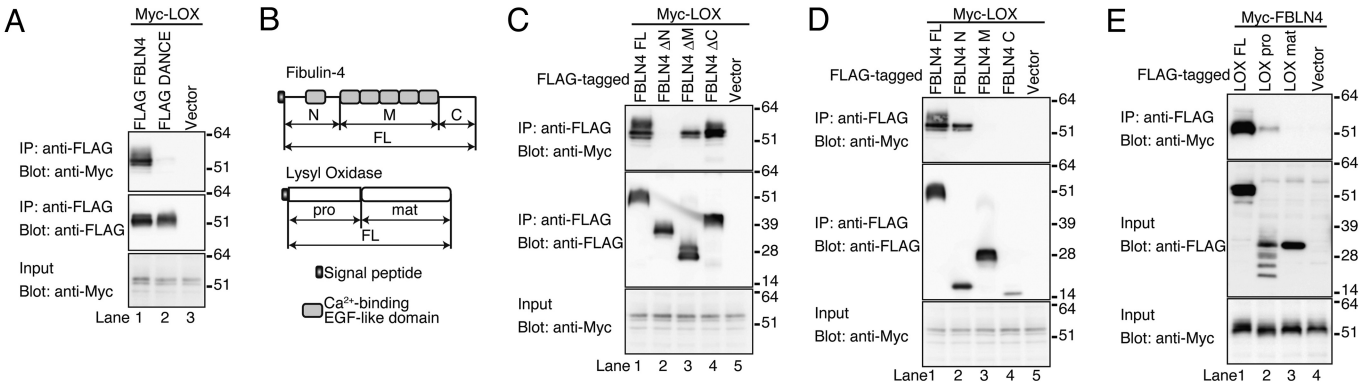

Fig. 5. The N-terminal domain of FBLN4 interacts with the propeptide domain of LOX. (*A*) FBLN4, but not DANCE, interacted with LOX measured by in vitro binding assay. Myc-tagged LOX was coprecipitated with FLAG-tagged FBLN4 (lane 1), but not with FLAG-tagged DANCE (lane 2). (*B*) Schematic representation of the domain composition of FBLN4 and LOX. C, C-terminal domain containing fibulin-type module; FL, full-length protein without endogenous signal peptide; M, tandem arrays of cbEGF domain; N, N-terminal domain; mat, mature catalytic LOX; pro, the propeptide of LOX. (*C*) Among deletion mutants, only FBLN4 ΔN could not interact with LOX (lane 2). (*D*) FBLN4 N domain interacted with LOX (lane 2), whereas M and C domains did not (lanes 3 and 4, respectively). (*E*) The propeptide of LOX interacted with FBLN4 (lane 2), whereas the mature LOX did not (lane 3). The LOX pro appeared as multiple bands due to glycosylation.

three domains (N, M, and C; Fig. 5*B*). An immunoprecipitation assay showed that only the mutant lacking the N-domain could not interact with Myc-tagged LOX (Fig. 5*C*, lane 2). To confirm the binding specificity, we performed immunoprecipitation experiments with truncated proteins. Consistent with the result with the deletion mutants, an assay using domain-only constructs of FBLN4 showed that only FLAG-tagged N-domain could interact with Myc-tagged LOX, whereas M- and C-domains could not (compare lane 2 with lanes 3 and 4 in Fig. 5*D*). These results indicate that the N-terminal domain of FBLN4 specifically interacts with LOX.

The immunoprecipitation assay using LOX truncated proteins also revealed that the propeptide region of LOX interacts with FBLN4, whereas mature LOX does not (Fig. 5*E*). Taking all of these results into account, we conclude that FBLN4 interacts with the propeptide of LOX through its N terminus domain.

FBLN4 Colocalizes with LOX on Elastic Fibers. To examine whether FBLN4 interacts with LOX in the course of elastic fiber assembly, we performed immunostaining of cultured human skin fibroblasts (HSFs) to visualize endogenously expressed FBLN4, LOX, and elastin. As shown in Fig. 6 *A* and *B*, FBLN4 colocalized both with LOX and elastin. Together with the direct binding of FBLN4 with LOX shown above and of FBLN4 with tropoelastin (31), these findings suggest that interaction of FBLN4 and LOX occurs during the process of elastic fiber assembly. Because both *Fbln4* null mice and *Lox* null mice exhibit markedly decreased amount of cross-linked elastin (31, 38), we reason that the direct interaction of these molecules have an important role in elastogenesis.

FBLN4 Tethers proLOX on Tropoelastin. To investigate the role of FBLN4 and LOX interaction in elastogenesis, a solid phase binding assay was performed. Tropoelastin-coated plates were incubated with full-length LOX (proLOX) with or without FBLN4. As shown in Fig. 6*C*, proLOX could not bind tropoelastin in the absence of FBLN4. However, when FBLN4 was added into the reaction buffer, proLOX bound to the plate, which suggests that FBLN4 tethers proLOX on tropoelastin.

Discussion

In the present study, we generated smooth muscle-specific *Fbln4* knockout mice, and found that a marked decrease (down to 18.5 ± 6.3%) of *Fbln4* expression in arteries of $Fbln4^{flox/flox}$ *Sm*+ mice causes defective postnatal development of elastic laminae, but the residual expression of *Fbln4* is sufficient for embryonic development of elastic laminae. Decreased expression of *Fbln4* to an even lower level in $Fbln4^{flox/null}$ *Sm*+ mice (8.4 ± 2.7%) resulted in aberrant embryonic development of elastic laminae and aneurysm of ascending aortae. We also found that FBLN4 recruits proLOX on tropoelastin via interaction with the propeptide of LOX, indicating that FBLN4 acts to place LOX in the proximity of its substrate, tropoelastin. The interaction with LOX was not observed for DANCE, suggesting that each FBLN has a distinct role in elastogenesis.

Considering the complete disruption of elastic laminae in $Fbln4^{null/null}$ (31) or $Fbln4^{\Delta Ex2/\Delta Ex2}$ neonates, it is of interest that $Fbln4^{flox/flox}$ *Sm*+ mice do not show impaired elastogenesis at P0, although *Sm22α-Cre* is expressed at 14.5 dpc when aortic elastic laminae start to develop, and the expression of FBLN4 in the aorta is largely eliminated by P0. An explanation for this discrepancy is that a small amount of residual FBLN4 may be sufficient for the embryonic development of elastic laminae. Another possibility is that FBLN4 secreted from remote organs, such as lungs, kidneys, and skeletal muscles, may act on developing arteries in an endocrine manner. In either case, our results demonstrate the requirement for FBLN4 in postnatal development of elastic laminae. The amount of insoluble elastin in the aortae of our conditional knockout mice appeared to be comparable with those of control mice in electron micrographs. This finding suggests that a small amount of FBLN4 (8%) is sufficient for the elastin cross-link, but is insufficient for proper assembly of elastin to form compact layers.

Another genetically engineered mouse mutant with reduced expression of FBLN4 has been described (42). Targeted disruption of the *Mus81* gene, which is located adjacent to the *Fbln4* gene, by insertion of a neo^r cassette resulted in $Fbln4^{R/R}$ mice with *Fbln4* mRNA expression reduced to ≈25% in embryonic fibroblast and to ≈40% in adult aorta compared with wild-type controls. These mice show dilated ascending aortae and tortuous descending aortae by 10 days after birth, although the reduction of *Fbln4* expression in aortae is much milder than in our $Fbln4^{flox/flox}$ *Sm*+ mice. The systemic reduction of *Fbln4* in tissues in $Fbln4^{R/R}$ mice may account for the more severe phenotype than that of our mice. It is still possible that the disruption of the *Mus81* gene influences the phenotype of $Fbln4^{R/R}$ mice, because Mus81 is an endonuclease implicated in maintaining genetic stability, although *Mus81* single knockout mice do not show gross abnormalities (43). Hanada et al. (42) suggested a relationship between the increase of TGFβ signaling and the development of aneurysm in $Fbln4^{R/R}$ mice. Further investigation is required to clarify whether augmented TGFβ signaling is involved in the aneurysm progression in our conditional knockout mice.

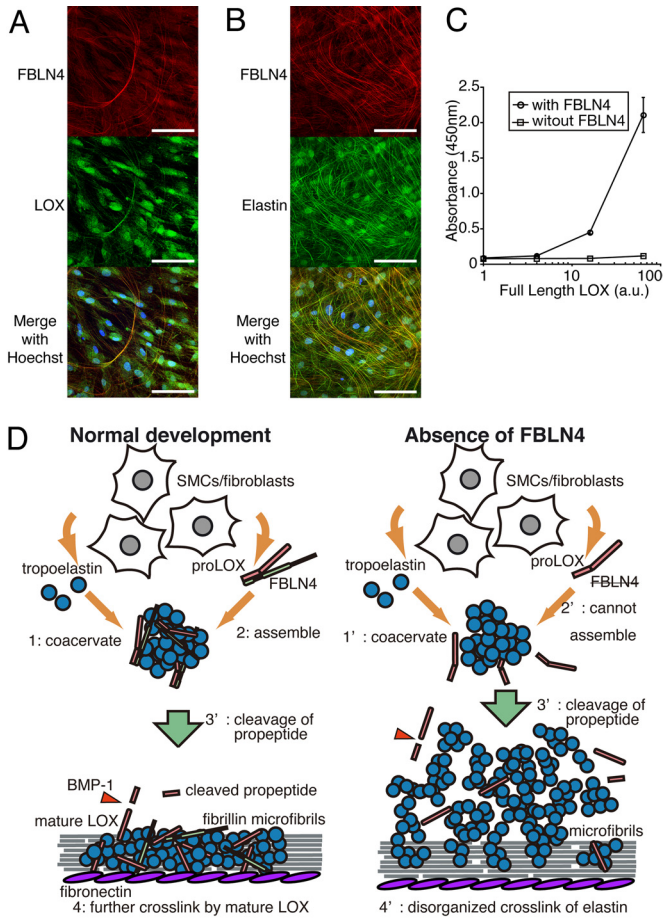

Fig. 6. FBLN4 tethers LOX to tropoelastin. (*A* and *B*) FBLN4 colocalized with both LOX and elastin on fibrillar structures in cultured HSFs. (Scale bar, 100 μm.) (*C*) Solid phase binding assays showed that full-length LOX deposited on tropoelastin-coated plates in the presence of FBLN4, but not in the absence of FBLN4. Data are represented as means ± SD of three independent experiments. (*D*) A proposed model for the role of interaction of FBLN4 and LOX in the elastic fiber assembly. (*Left*) Under normal condition, secreted tropoelastin coacervates to form small aggregates (*i*); FBLN4 tethers proLOX on these aggregates (*ii*); these ternary complexes deposit on microfibrills and the propeptide of proLOX is cleaved by BMP1 producing mature LOX (*iii*); tropoelastin monomers are cross-linked to each other by mature LOX to produce functional elastic laminae (*iv*). (*Right*) However, in the absence of FBLN4, tropoelastin molecules coacervate (*i'*) but proLOX cannot assemble to the aggregates (*ii'*); therefore, LOX cannot cross-link tropoelastin aggregates effectively even though they may be cleaved into mature form (*iii'*); which leads to disorganized elastic laminae (*iv'*). SMCs, smooth muscle cells.

Mutations of the human *FBLN4* gene have been recently reported. A compound heterozygous *FBLN4* mutant was recently described to show cutis laxa, aneurysm restricted to the ascending aorta, and tortuous arteries, with severe reduction of the tissue content of elastic fibers (44). Another human *FBLN4* missense mutation was reported to result in cutis laxa, vascular tortuosity, ascending aortic aneurysm, emphysema, and diaphragmatic hernia with underdeveloped elastic tissues (32). These arterial symptoms found in humans are consistent with the phenotypes of our *Fbln4* conditional knockout mice.

In elastic fiber assembly, LOX has a crucial role. It has been reported that the propeptide of LOX is required to direct LOX on elastic fibers in cell culture (37). In this study, however, both the prodomain and mature catalytic domain interacted with tropoelastin as monitored by ligand blot and mammalian two-hybrid assays. Therefore, it was not clear why the propeptide, not the catalytic domain, is necessary for LOX deposition onto elastic fibers. In the present study, we found that the LOX propeptide, not its catalytic domain, specifically interacts with FBLN4 (Fig. 5*E*). Solid-phase binding assays revealed that FBLN4 facilitates the deposition of proLOX on tropoelastin, whereas proLOX alone cannot deposit on tropoelastin (Fig. 6*C*). From these data, together with our previous data showing direct binding of FBLN4 and tropoelastin (31), we propose a model for the role of FBLN4: FBLN4 recruits LOX to elastic fibers by tethering proLOX to tropoelastin; thus, facilitating tropoelastin cross-linking (Fig. 6*D*). In this model, proLOX is cleaved to be activated in the vicinity of its substrate, tropoelastin, which may explain why active LOX are not scattered in the extracellular space to form unwanted cross-links. This model is further supported by previously reported findings that in $Fbln4^{null/null}$ mice, desmosine content was reduced to 6% of wild-type mice, although the expression of LOX and elastin was not altered, indicating a requirement for FBLN4 in the proper cross-linking reaction (31).

Recently, it was reported that full-length LOX interacts with FBLN4 and that fibrillin-1 inhibits the interaction of these proteins (45). In this study, Choudhury et al. (45) also showed using BIAcore that interaction of FBLN4 and tropoelastin was enhanced in the presence of full-length LOX. These findings, together with our results, emphasize the importance of the ternary complex of FBLN4, LOX, and tropoelastin in the process of elastic fiber assembly.

Because there are many molecules involved in elastogenesis, we cannot exclude the possibility that the observed requirement for FBLN4 reflects the participation of other extracellular molecules. For example, as FBLN4 binds to DANCE (45), the reduced expression of FBLN4 may affect the function of DANCE. The larger requirement for FBLN4 in postnatal development may reflect the different expression pattern of LOX families during the pre and postnatal development. Further studies will be required to test these hypotheses.

In summary, we found that FBLN4 is required in the postnatal development of arterial elastic laminae, and the dose requirement of FBLN4 is larger in postnatal development than in embryogenesis. FBLN4 tethers LOX to tropoelastin through the interaction with the LOX propeptide, which illustrates a specific role for FBLN4 in promoting the proper maturation of elastic fibers. FBLN4 might be an agent to treat age-related pathologic conditions that are related to elastic fiber degradation, for example, aortic aneurysm.

Methods

Generation of Fbln4 Conditional Knockout Mice. The exon 2 of mouse *Fbln4* was flanked by two *loxP* sequences inserted in intron 1 and 2. To generate vascular smooth muscle specific *Fbln4* conditional knockout mice, $Fbln4^{flox/+}$ mice were crossed with transgenic mice expressing Cre recombinase under control of the *Sm22*α promoter (The Jackson Laboratory) (40, 41). To generate systemically exon 2-deleted mice ($\Delta Ex2$), $Fbln4^{flox/+}$ mice were crossed with *Ayu-1 Cre* knockin mice (46, 47). For details, see *SI Methods*. All animals were maintained and all experiments were performed in accordance with the Regulation on Animal Experimentation at Kyoto University.

Tissue RNA Extraction and Quantitative PCR. Total RNA was extracted using TRIzol reagent (Invitrogen) and transcribed to cDNA with random hexamers using the SuperScript III First-Strand Synthesis System (Invitrogen). For quantitative PCR, the reaction was performed with a QuantiFAST SYBR Green PCR kit (QIAGEN), and the products were analyzed with the DNA Engine Opticon (Bio-Rad). Expression levels of *Gapdh* transcripts were used to normalize the cDNA levels. Data are presented as means ± SD of several independent experiments each performed in duplicate. Primer sequences used for quantitative PCR are provided in Table S2.

Pressure-Diameter Relationship. The aortae were excised, and the aorta dimensions and the intraaortic pressure were simultaneously recorded as previously described (24). Numbers of studied mice are indicated in each figure. The slope of

each curve was calculated from the aortic dimension at 40-mm Hg and 120-mm Hg. For details, see *SI Methods*.

In Vitro Binding Assay. Recombinant Myc-LOX or Myc-FBLN4 proteins were mixed with a set of FLAG-tagged proteins, and each mixture was subjected to immunoprecipitation with anti-FLAG M2 affinity gel (Sigma) followed by SDS/PAGE and Western blotting as described previously (26). Expression vectors of truncated mutants were constructed by amplifying cDNA as a template. Primer sequences used for PCR are provided in Table S3. For details, see *SI Methods*.

Immunocytochemistry. HSFs, which were taken from the facial skin of a 3-month-old baby, were kindly provided by M. Naito (Kyoto University). HSFs were cultured on microscope cover glasses (Fisherbrand) and were stained as previously described (26). The primary antibodies used were anti-LOX (NB-100-2530; Novus Biologicals), anti-elastin (PR533; EPC), and anti-FBLN4 (9C10) antibodies. The secondary antibodies used were AlexaFluor 488-conjugated anti-rabbit and AlexaFluor 546-conjugated anti-mouse IgG antibodies (Invitrogen), followed by nuclear staining with Hoechst 33258 (Dojindo). For details, see *SI Methods*.

Solid-Phase Binding Assay. Solid-phase binding assays using purified tropoelastin were performed as described previously with some modifications (31). As soluble ligands, conditioned media of HEK293T cells transfected with a mammalian expression vector encoding FLAG-tagged full length LOX were used. Conditioned media were harvested and concentrated 10-fold by ultrafiltration in Centricon Ultracel YM-10 (Millipore). The concentrated sample was serially diluted with Tris-buffered saline containing 2% skim milk with 2 mM $CaCl_2$, with or without 40 μg/mL of recombinant FBLN4. These mixtures were used as ligands for the assay. Data are presented as means $\pm$ SD of three independent experiments. For details, see *SI Methods*.

Statistical Analyses. Statistical analyses were performed with unpaired *t* test. $P < 0.05$ was considered to be significant.

ACKNOWLEDGMENTS. We thank Ms. Naoko Tomikawa and Ms. Akemi Yoshioka for their excellent technical assistance; Neal G. Copeland (Institute of Molecular and Cell Biology, Singapore) for defective prophage λ-Red recombineering system; Junji Takeda (Osaka University, Osaka, Japan) and Kosuke Yusa (Osaka University, Osaka, Japan) for plasmid containing *FRT*-flanked *neo*-cassette; Ken-ichi Yamamura (Kumamoto University, Kumamoto, Japan) and Kimi Araki (Kumamoto University, Kumamoto, Japan) for *Ayu-1 Cre* expressing mice; Shigehiko Suzuki (Kyoto University, Kyoto, Japan) and Motoko Naito (Kyoto Univeristy, Kyoto, Japan) for HSFs; and Yoshinobu Toda (Kyoto University, Kyoto, Japan) for tissue preparation and EVG staining. This work was supported by grants from the Japan Society for the Promotion of Science, and the Ministry of Education, Culture, Sports, Science, and Technology (to T.N. and M.H.); the Japan Science and Technology Agency, the Takeda Science Foundation, the Uehara Memorial Foundation, the Naito Foudation, and the Japan Health Foundation (to T.N.); and the Cell Science Research Foundation, the Nakatomi Foundation, Mitsui Sumitomo Insurance Welfare Foundation, and Japan Foundation of Cardiovascular Research (to M.H.).

1. Rosenbloom J, Abrams WR, Mecham R (1993) Extracellular matrix 4: The elastic fiber. *FASEB J* 7:1208–1218.
2. Bailey AJ (2001) Molecular mechanisms of ageing in connective tissues. *Mech Ageing Dev* 122:735–755.
3. Pasquali-Ronchetti I, Baccarani-Contri M (1997) Elastic fiber during development and aging. *Microsc Res Tech* 38:428–435.
4. Sakai LY, Keene DR, Engvall E (1986) Fibrillin, a new 350-kD glycoprotein, is a component of extracellular microfibrils. *J Cell Biol* 103:2499–2509.
5. Zhang H, et al. (1994) Structure and expression of fibrillin-2, a novel microfibrillar component preferentially located in elastic matrices. *J Cell Biol* 124:855–863.
6. Ramirez F, Sakai LY, Dietz HC, Rifkin DB (2004) Fibrillin microfibrils: Multipurpose extracellular networks in organismal physiology. *Physiol Genomics* 19:151–154.
7. Gray WR, Sandberg LB, Foster JA (1973) Molecular model for elastin structure and function. *Nature* 246:461–466.
8. Wagenseil JE, Mecham RP (2007) New insights into elastic fiber assembly. *Birth Defects Res C Embryo Today* 81:229–240.
9. Gibson MA, et al. (1996) Further characterization of proteins associated with elastic fiber microfibrils including the molecular cloning of MAGP-2 (MP25). *J Biol Chem* 271:1096–1103.
10. Gibson MA, Hughes JL, Fanning JC, Cleary EG (1986) The major antigen of elastin-associated microfibrils is a 31-kDa glycoprotein. *J Biol Chem* 261:11429–11436.
11. Bressan GM, Castellani I, Colombatti A, Volpin D (1983) Isolation and characterization of a 115,000-dalton matrix-associated glycoprotein from chick aorta. *J Biol Chem* 258:13262–13267.
12. Bressan GM, et al. (1993) Emilin, a component of elastic fibers preferentially located at the elastin-microfibrils interface. *J Cell Biol* 121:201–212.
13. Huang G, et al. (2009) Fibronectin binds and enhances the activity of bone morphogenetic protein 1. *J Biol Chem* 284:25879–25888.
14. Sabatier L, et al. (2009) Fibrillin assembly requires fibronectin. *Mol Biol Cell* 20:846–858.
15. Hirai M, et al. (2007) Latent TGF-beta-binding protein 2 binds to DANCE/fibulin-5 and regulates elastic fiber assembly. *EMBO J* 26:3283–3295.
16. Sterner-Kock A, et al. (2002) Disruption of the gene encoding the latent transforming growth factor-beta binding protein 4 (LTBP-4) causes abnormal lung development, cardiomyopathy, and colorectal cancer. *Genes Dev* 16:2264–2273.
17. Argraves WS, Greene LM, Cooley MA, Gallagher WM (2003) Fibulins: Physiological and disease perspectives. *EMBO Rep* 4:1127–1131.
18. de Vega S, et al. (2007) TM14 is a new member of the fibulin family (fibulin-7) that interacts with extracellular matrix molecules and is active for cell binding. *J Biol Chem* 282:30878–30888.
19. Nakamura T, et al. (1999) DANCE, a novel secreted RGD protein expressed in developing, atherosclerotic, and balloon-injured arteries. *J Biol Chem* 274:22476–22483.
20. Lecka-Czernik B, Lumpkin CK, Jr, Goldstein S (1995) An overexpressed gene transcript in senescent and quiescent human fibroblasts encoding a novel protein in the epidermal growth factor-like repeat family stimulates DNA synthesis. *Mol Cell Biol* 15:120–128.
21. Stone EM, et al. (1999) A single EFEMP1 mutation associated with both Malattia Leventinese and Doyne honeycomb retinal dystrophy. *Nat Genet* 22:199–202.
22. McLaughlin PJ, et al. (2007) Lack of fibulin-3 causes early aging and herniation, but not macular degeneration in mice. *Hum Mol Genet* 16:3059–3070.
23. Kowal RC, Richardson JA, Miano JM, Olson EN (1999) EVEC, a novel epidermal growth factor-like repeat-containing protein upregulated in embryonic and diseased adult vasculature. *Circ Res* 84:1166–1176.
24. Nakamura T, et al. (2002) Fibulin-5/DANCE is essential for elastogenesis in vivo. *Nature* 415:171–175.
25. Yanagisawa H, et al. (2002) Fibulin-5 is an elastin-binding protein essential for elastic fibre development in vivo. *Nature* 415:168–171.
26. Hirai M, et al. (2007) Fibulin-5/DANCE has an elastogenic organizer activity that is abrogated by proteolytic cleavage in vivo. *J Cell Biol* 176:1061–1071.
27. Loeys B, et al. (2002) Homozygosity for a missense mutation in fibulin-5 (FBLN5) results in a severe form of cutis laxa. *Hum Mol Genet* 11:2113–2118.
28. Markova D, et al. (2003) Genetic heterogeneity of cutis laxa: A heterozygous tandem duplication within the fibulin-5 (FBLN5) gene. *Am J Hum Genet* 72:998–1004.
29. Stone EM, et al. (2004) Missense variations in the fibulin 5 gene and age-related macular degeneration. *N Engl J Med* 351:346–353.
30. Giltay R, Timpl R, Kostka G (1999) Sequence, recombinant expression and tissue localization of two novel extracellular matrix proteins, fibulin-3 and fibulin-4. *Matrix Biol* 18:469–480.
31. McLaughlin PJ, et al. (2006) Targeted disruption of fibulin-4 abolishes elastogenesis and causes perinatal lethality in mice. *Mol Cell Biol* 26:1700–1709.
32. Hucthagowder V, et al. (2006) Fibulin-4: A novel gene for an autosomal recessive cutis laxa syndrome. *Am J Hum Genet* 78:1075–1080.
33. Xiang Y, et al. (2006) Fibulin-4 is a target of autoimmunity predominantly in patients with osteoarthritis. *J Immunol* 176:3196–3204.
34. Lucero HA, Kagan HM (2006) Lysyl oxidase: An oxidative enzyme and effector of cell function. *Cell Mol Life Sci* 63:2304–2316.
35. Kagan HM, Li W (2003) Lysyl oxidase: Properties, specificity, and biological roles inside and outside of the cell. *J Cell Biochem* 88:660–672.
36. Uzel MI, et al. (2001) Multiple bone morphogenetic protein 1-related mammalian metalloproteinases process pro-lysyl oxidase at the correct physiological site and control lysyl oxidase activation in mouse embryo fibroblast cultures. *J Biol Chem* 276:22537–22543.
37. Thomassin L, et al. (2005) The Pro-regions of lysyl oxidase and lysyl oxidase-like 1 are required for deposition onto elastic fibers. *J Biol Chem* 280:42848–42855.
38. Hornstra IK, et al. (2003) Lysyl oxidase is required for vascular and diaphragmatic development in mice. *J Biol Chem* 278:14387–14393.
39. Maki JM, et al. (2002) Inactivation of the lysyl oxidase gene Lox leads to aortic aneurysms, cardiovascular dysfunction, and perinatal death in mice. *Circulation* 106:2503–2509.
40. Holtwick R, et al. (2002) Smooth muscle-selective deletion of guanylyl cyclase-A prevents the acute but not chronic effects of ANP on blood pressure. *Proc Natl Acad Sci USA* 99:7142–7147.
41. Li L, Miano JM, Mercer B, Olson EN (1996) Expression of the SM22alpha promoter in transgenic mice provides evidence for distinct transcriptional regulatory programs in vascular and visceral smooth muscle cells. *J Cell Biol* 132:849–859.
42. Hanada K, et al. (2007) Perturbations of vascular homeostasis and aortic valve abnormalities in fibulin-4 deficient mice. *Circ Res* 100:738–746.
43. Dendouga N, et al. (2005) Disruption of murine Mus81 increases genomic instability and DNA damage sensitivity but does not promote tumorigenesis. *Mol Cell Biol* 25:7569–7579.
44. Dasouki M, et al. (2007) Compound heterozygous mutations in fibulin-4 causing neonatal lethal pulmonary artery occlusion, aortic aneurysm, arachnodactyly, and mild cutis laxa. *Am J Med Genet A* 143A:2635–2641.
45. Choudhury R, et al. (2009) Differential regulation of elastic fiber formation by fibulins -4 AND -5. *J Biol Chem* 284:24553–24567.
46. Morita M, et al. (2003) HLF/HIF-2alpha is a key factor in retinopathy of prematurity in association with erythropoietin. *EMBO J* 22:1134–1146.
47. Niwa H, et al. (1993) An efficient gene-trap method using poly A trap vectors and characterization of gene-trap events. *J Biochem* 113:343–349.